Journal of ETA Maritime Science 2024;12(1):83-91

Model Validation and Hydrodynamic Performance of an Oscillating Buoy Wave Energy Converter

Giri Ram[1], Mohd Rashdan Saad[1], Noh Zainal Abidin[2], Mohd Rosdzimin Abdul Rahman[1]

[1]Universiti Pertahanan Nasional Malaysia, Faculty of Engineering, Department of Mechanical Engineering, Kuala Lumpur, Malaysia
[2]Universiti Pertahanan Nasional Malaysia, Faculty of Defence Science and Technology, Department of Science and Maritime Technology, Kuala Lumpur, Malaysia

Abstract

An oscillating buoy (OB) could function simultaneously as a wave energy converter and a breakwater. In this work, a numerical study is conducted to assess the ability of the buoy to perform both aforementioned tasks by quantitatively and qualitatively assessing its hydrodynamic performance. The computational fluid dynamics solver used for the numerical study is ANSYS Fluent, which uses Reynolds-averaged Navier-Stokes equations and Volume of Fluid method for the design and simulation of the numerical model, which consists of a rectangular OB that floats on the surface of a numerical wave tank. First, a total of six independent studies, namely the time, meshing, damping, overset geometry, flow viscosity, and spatial studies, were conducted for validation purposes. Second, calculation and analysis of the heave and transmission coefficients and vorticity magnitude were conducted to assess the hydrodynamic performance. Results of independent studies show cases with a high degree of accuracy to the experimental model, whereas results for hydrodynamic performance show a generally increasing heave movement of OB and transmission coefficient across the range of wave periods studied. Meanwhile, the vorticity magnitude flow fields show at least two vortices for all wave periods studied, except for the shortest two wave periods.

Keywords: Computational fluid dynamics, Wave energy converter, Oscillating buoy, Breakwater, Hydrodynamic performance

1. Introduction

Considering the urgent need to address the issue of climate change, most countries have pledged to go net-zero carbon in terms of emissions by 2050. One way to do so is to replace non-renewables with renewable energy sources, and wave energy is a key component in the mix of renewable energies. It is seen to be the preferred source of energy for remote and island regions that are difficult to access through the national grid system [1] but have abundant ocean wave energy potential from the nearby ocean.

Wave energy converters (WEC), which convert wave energy to electrical energy, come in various types, such as oscillating bodies, overtopping devices, and oscillating water columns. An oscillating buoy (OB) is a type of oscillating body that either floats or is submerged in the ocean and works based on translational (heave) or rotational movement [2]. The system bypasses the secondary conversion process that uses a power take-off unit, typically found in other types of WECs, by direct drive to a linear electrical generator [3]. Aside from its electrical energy-generating properties, the OB could also act as a breakwater, which is a protective barrier between ocean waves and coastal infrastructure, which could experience frequent wear and tear due to the constant barrage of ocean waves. This hybrid use of the device makes it more space-efficient and cost-effective than single-use ocean devices.

The validation study serves the purpose of creating a numerical model that can accurately replicate real-life conditions either in a controlled experimental setup or in an open environment. In the case of a numerical model consisting of a floating body that is subjected to wave oscillations, the level of accuracy could vary depending on

Address for Correspondence: Giri Ram, Universiti Pertahanan Nasional Malaysia, Faculty of Engineering, Department of Mechanical Engineering, Kuala Lumpur, Malaysia
E-mail: ramamethyst@gmail.com
ORCID ID: orcid.org/0000-0002-9970-861X

Received: 23.08.2023
Last Revision Received: 14.12.2023
Accepted: 19.01.2024

To cite this article: G. Ram, M. R. Saad, N. Z. Abidin, and M. R. A. Rahman. "Model Validation and Hydrodynamic Performance of an Oscillating Buoy Wave Energy Converter." *Journal of ETA Maritime Science*, vol. 12(1), pp. 83-91, 2024.

the technique used. One technique is smoothed-particle hydrodynamics, which is a mesh-free approach that uses an array of particles to form a simulation domain [4]. In addition, a layering technique was used by Luo et al. [5], where dynamic layering to add or remove meshes next to a moving boundary was used. Gomes et al. [6] also used layering, wherein the inlet acted as a moving wall. Other techniques include smoothing and remeshing. Ringe [7] used both techniques to model a one-directional wave tank.

A relatively newer technique for modeling moving bodies is the overset mesh technique, which works based on the principle that two separate mesh regions move relative to each other while having a static internal condition with fixed mesh connectivity [8]. Zhang et al. [9] used the overset mesh technique because of its better accuracy for large-scale deformations compared with the dynamic mesh. Lakshmynarayana [10] also used overset grids, which are attached to a floating body and move with it freely according to the motion response.

The hydrodynamic performance of WEC has been studied extensively and is typically assessed using several coefficients that are calculated based on measurements of various waves, pressure, velocity, and other gages installed in the wave tank. In the case of an OB, the coefficient related to heave movement provides an understanding of the level of wave energy that is converted to electrical energy. Cheng et al. [11] experimentally and numerically studied a hybrid WEC-breakwater system, where the breakwater, in the form of an OB, is subjected to a heave-only motion and the heaving displacement and velocity of the OB are analyzed.

In addition to the quantitative analysis of heave movement, qualitative analysis in the form of velocity flow fields allows for the detection of energy loss in the system in the form of vortices, as studied by Zhang et al. [12]. On the other hand, the calculation of the transmission coefficient determines the ability of the OB to act as a breakwater, as shown by Ji et al. [13], who studied the effects of variations in draft, wave frequency, and curtain height of a heaving WEC-breakwater device on the transmission coefficient.

This study can be divided into two parts. The first part involves a validation study whereby a total of six independent studies, concerning the time, spatial, mesh, numerical beach, overset mesh design, and viscosity model, are conducted on a rectangular buoy. In the second part, the hydrodynamic performance of the OB, concerning its ability to generate wave power and act as a breakwater, is studied.

A novelty of this study is that six independent studies were conducted to develop an accurate numerical model. Besides that, to the best knowledge of the authors, a comprehensive study on the vorticity magnitude flow fields, because of the interaction of waves at the surface of water body and OB, for different wave periods and cycles, has not been published before.

2. Numerical Model

2.1. Governing Equations

Numerical modeling and simulations were carried out using ANSYS 2023 R2: Fluent, a computational fluid dynamics solver that works according to the finite volume method, wherein regions of interest are segmented into sub-regions and governing equations are discretised and solved iteratively over every sub-region [6]. The simulation was performed using an Intel(R) Xeon(R) Platinum 8260 CPU @ 2.40 GHz and 2.39 GHz (two processors) with 128 GB of RAM. A total of 45 parallel processors were used during the simulation.

Reynolds-averaged Navier-Stokes equations were used in the system along with some additional variables. Equations 1-3 show the mass continuity and Navier-Stokes equations [14].

$$\frac{\partial(\rho u)}{\partial x}+\frac{\partial(\rho v)}{\partial y}=0 \tag{1}$$

$$\rho\left(\frac{\partial u}{\partial t}+u\frac{\partial u}{\partial x}+v\frac{\partial u}{\partial y}\right)=-\frac{\partial p}{\partial x}+2\mu\frac{\partial^2 v}{\partial y^2} +\frac{\partial}{\partial y}\left(\mu\left(\frac{\partial u}{\partial y}+\frac{\partial v}{\partial x}\right)\right)+F_x \tag{2}$$

$$\rho\left(\frac{\partial v}{\partial t}+u\frac{\partial v}{\partial x}+v\frac{\partial v}{\partial y}\right)=-\frac{\partial p}{\partial x}+2\mu\frac{\partial^2 u}{\partial y^2} +\frac{\partial}{\partial x}\left(\mu\left(\frac{\partial u}{\partial y}+\frac{\partial v}{\partial x}\right)\right)-\rho g+F_y \tag{3}$$

Volume of fluid method was used to simulate an immiscible, multiphase mixture. The scale of the model is considered to be small, where air and water compressibility are assumed to be negligible.

To evaluate the results of independent studies, heave movement, wave elevation, and flow time calculations are plotted as per Equations 4-6. The relative error of the present cases relative to the experimental data is calculated as per Equation (7) [15].

$$\textit{normalized heave movement}=\frac{Z}{d} \tag{4}$$

$$\textit{normalized wave elevation}=\frac{\eta}{d} \tag{5}$$

$$normalized\ flow\ time = \frac{t}{T} \quad (6)$$

$$error = \frac{\epsilon_{Numerical} - \epsilon_{Experimental}}{\epsilon_{Experimental}} \text{ x } 100 \quad (7)$$

To calculate the performance of the OB, the heave coefficient and transmission coefficient are calculated as per Equations 8 and 9 respectively.

$$Ch = \frac{A_{Heave}}{A_{Incident}} \quad (8)$$

$$Ct = \frac{A_{Transmission}}{A_{Incident}} \quad (9)$$

2.2. Numerical Wave Tank (NWT)

The layout of the model along with dimensions and applied labels during boundary conditions is shown in Figure 1. The dimensions of the two-dimensional NWT were set to 18 m x 0.8 m, where the point of origin is at the centroid of the domain. Therefore, the water depth is 0.4 m, which is similar to the experimental setup used by He et al. [16] and the numerical model used by Lyu et al. [17].

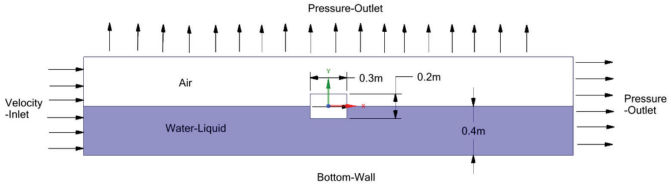

Figure 1. *Two-dimensional schematic of NWT with added rectangular buoy and details of dimensions, phases, and boundary types*

NWT: Numerical wave tank

The OB was partially immersed in still water, has dimensions of 0.3 m x 0.3 m x 0.2 m, and is located at the center of the background (Figure 1). Two phases, namely air and water-liquid phase, were selected as shown in Table 1. The boundary and initial conditions are shown in Table 2. The wave theory is selected in accordance with the graph for limits of validity for wave theories [18].

2.3. Validation

The six independent studies conducted for validation are time, mesh, numerical beach, overset geometry, viscosity model, and spatial studies. For heave movement, an NWT with a rectangular buoy was used for simulation, whereas for wave elevation, an empty NWT was used, where the result of WG0 was compared with experimental data, except for spatial study.

Table 1. *Properties of the phases*

Material name	Density (kg/m^3)	Viscosity (kg/ms)
Air	1.225	1.789x10-3
Water-Liquid	1000	1003x10-3

Table 2. *Setting the boundary condition*

Description	Value
Free surface level (m)	0
Depth (m)	-0.4
Wave boundary condition option	Shallow/Intermediate waves
Wave theory	Third-order stokes
Wave height (m)	0.1
Wavelength (m)	1.9897
Operating pressure (Pa)	101325
Operating density (kg/m^3)	1.225
Wave period (rad/s)	1.2

A time study was conducted to assess the flow time at which wave elevation attains stability. The simulation was allowed to run until 126 s and results of 6 s range, between 30 s intervals was collected. Second, the mesh study involves coarse mesh with bias and fine mesh with bias, as shown in Figure 2a and b, respectively. To reduce computational time for coarse mesh, a biased mesh was used whereby Δx =0.015 m with a bias factor of 1.2, while Δy =0.015 m with a bias factor of 5 was set. Face meshing was used to attain a more uniform, hexahedron-shaped mesh.

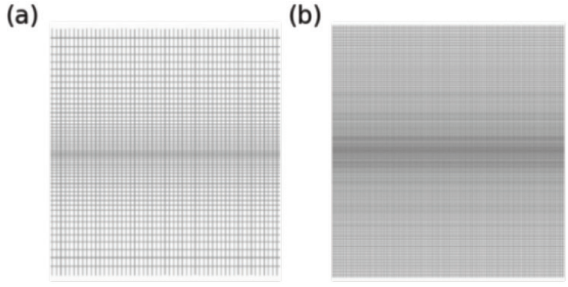

Figure 2. *Schematic of (a) coarse mesh with bias and (b) fine mesh with bias*

Lyu et al. [17] found that a mesh of Δx =0.02 m and below and Δz =0.01 m and below improved the reading on the maximum crest compared to mesh Δx =0.06 m and Δz =0.02 m. The coarse mesh case has a mesh structure that is comparable to the meshes improved by Lyu et al. [17]. As for the fine mesh, the element size is three times smaller at Δx and Δy of 0.005 m (Table 3).

Table 3. *Details of the mesh study*

Mesh type	Mesh Size (m)	Number of cells
Coarse	0.015	64800
Fine	0.005	576000

Third, the beaching effect in a wave tank prevents wave reflection from the outlet, thereby not distorting the measurements. Typically, a slope produces the beaching effect in experimental studies; however, in numerical studies, a numerical beach could also perform a similar task. Three numerical beach lengths from the outlet were tested.

The OB is subjected to heave movement using the overset mesh technique. It works based on the principle that two separate mesh regions move relative to each other while having a static internal condition with fixed mesh connectivity [8]. For the overset design study, circular and rectangular overset meshes were compared for their accuracy with experimental data.

In the flow viscosity study, laminar, standard k-epsilon, and Shear Stress Transport (SST) k-omega turbulence models were studied. These are commonly used viscosity models, based on the Windt et al. [8] study, where 41% of studies did not disclose model type, 18% used standard k-epsilon model, 13% SST k-omega, 10% laminar, 7% re-normalization group k-epsilon, 4% inviscid, and 5% others.

Finally, a spatial study looks into wave elevation at different locations from the inlet to the OB. A total of nine wave gages (shown in Figure 3), based on their distance to the point of origin, were used to measure wave elevation. Through this study, the characteristics of wave propagation can be observed.

2.4. Hydrodynamic Performance

To assess the ability of the OB to convert wave energy into useful electrical energy, the heave coefficient is calculated and compared for various wave periods. Second, the ability of the OB to function as a breakwater and reduce the amount of wave energy transmitted downstream of the OB is assessed using the calculated transmission coefficient. Finally, vorticity magnitude, which refers to the magnitude of spinning motion, is visualized in a velocity flow field diagram to detect vortices in the water phase and the magnitude of vorticity.

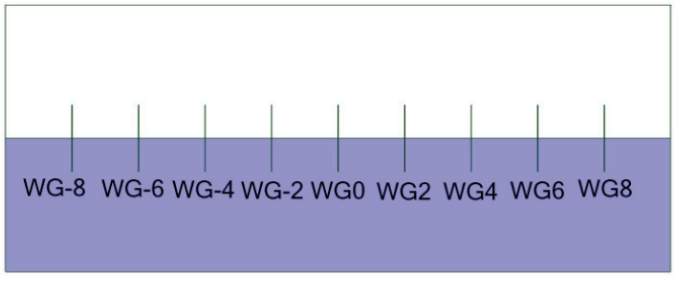

Figure 3. *Schematic of the wave gage location in NWT*

NWT: Numerical wave tank

3. Results and Discussion

3.1. Validation

The result for heave movement is shown in Figure 4, wave elevation in Figure 5, and the percentage of error relative to the experimental data is shown in Figure 6. For the time study, shown in Figures 4a, 5a, and 6a, the lowest error is seen to be for time ranges of 40-46 s and 50-56 s for both heave movement and wave elevation, respectively. Beyond the flow time of 56 s, the computing time was deemed too long and taxing for the computer. The results of relative error show that heave movement more accurately replicates experimental data compared to wave elevation, and that the optimal accuracy was found for the flow time range 50-56 s. This result is similar to the findings of Jiang et al. [19], where a steady state is observed between flow times of 40 s and 60 s.

For the results of the mesh study, shown in Figures 4b, 5b, and 6b, all cases show good accuracy to the experimental data, at a maximum error of 6% for the heave movement of the coarse mesh. This means that the coarse mesh case is favorable compared to the fine mesh case because of the reduced computing time. For the results of the spatial study, WG-2 shows a predictably shorter amplitude compared to WG-8, WG-6, and WG-4 because of its distance from the inlet and interference from wave reflection from the OB. Findings by Ji et al. [13] show that coarser meshes agree well with finer meshes for heave motion, but show little difference in peak and trough for wave elevations. This study shows the opposite result, where a higher similarity and accuracy to the experimental data is found for wave elevation compared to heave motion.

The results of the numerical beach study are shown in Figures 4c, 5c, and 6c. A higher irregularity in wave propagation could be observed for the no beach case compared with the beach cases, despite the lower error for heave movement. The optimal value for both heave and wave elevation was observed to be the beach 7-9 m case. Besides the numerical beach, a common method for wave absorption is to design a slope at the outlet. Ringe [7] studied the wave absorption of slopes with different steepness levels, perforated screens, and step-up absorbers and observed that the steepest slope with a 1:3 ratio showed the best result.

Both circular and rectangular overset designs show a low percentage of error (as shown in Figures 4d, 5d, and 6d). However, the rectangular overset case shows almost half the % of errors and is therefore considered to be more accurate in replicating the experimental results.

The viscosity model study (shown in Figures 4e, 5e, and 6e) shows a high accuracy for the laminar model compared to the SST k-omega and standard k-epsilon turbulence models.

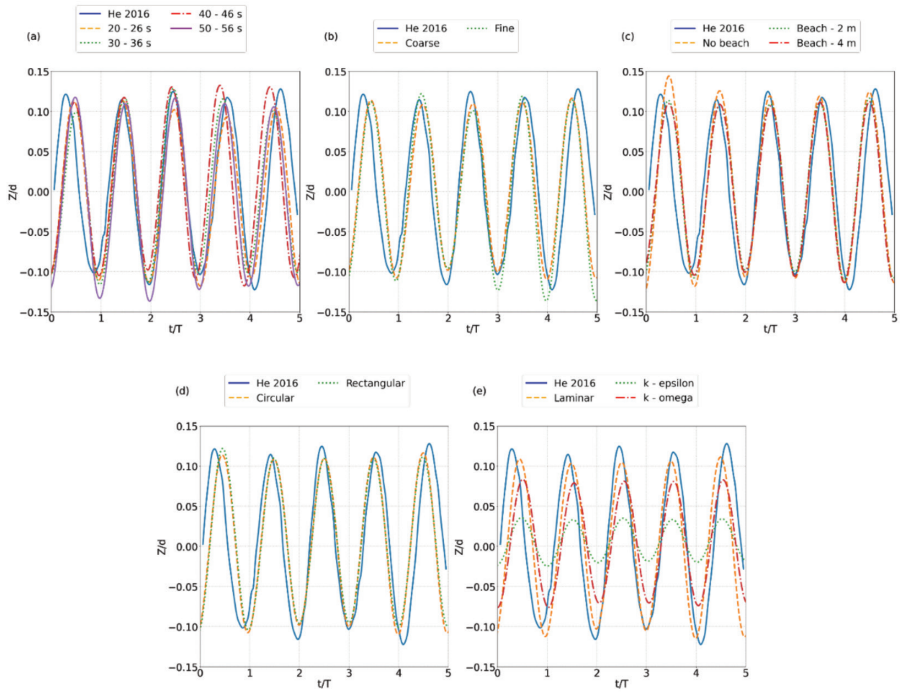

Figure 4. *Comparison of normalized heave movement versus normalized time between experimental data [16] and various cases of a) time study, b) mesh study, c) numerical beach study, d) overset geometry study, and e) viscosity study*

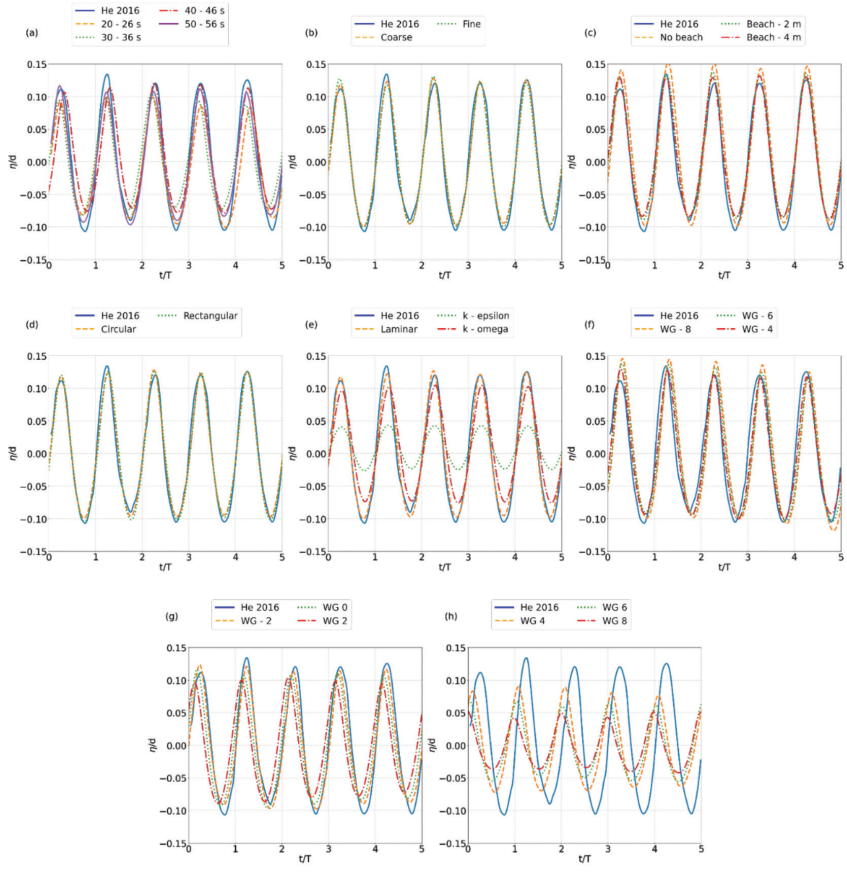

Figure 5. *Comparison of normalized wave elevation versus normalized time between experimental data [16] and various cases of a) time study, b) mesh study, c) numerical beach study, d) overset geometry study, e) viscosity study, f) spatial study for wave gauges WG-8, WG-6, and WG-4, g) spatial study for wave gages WG-2, WG0, and WG2, and h) spatial study for wave gauges WG4, WG6, and WG8*

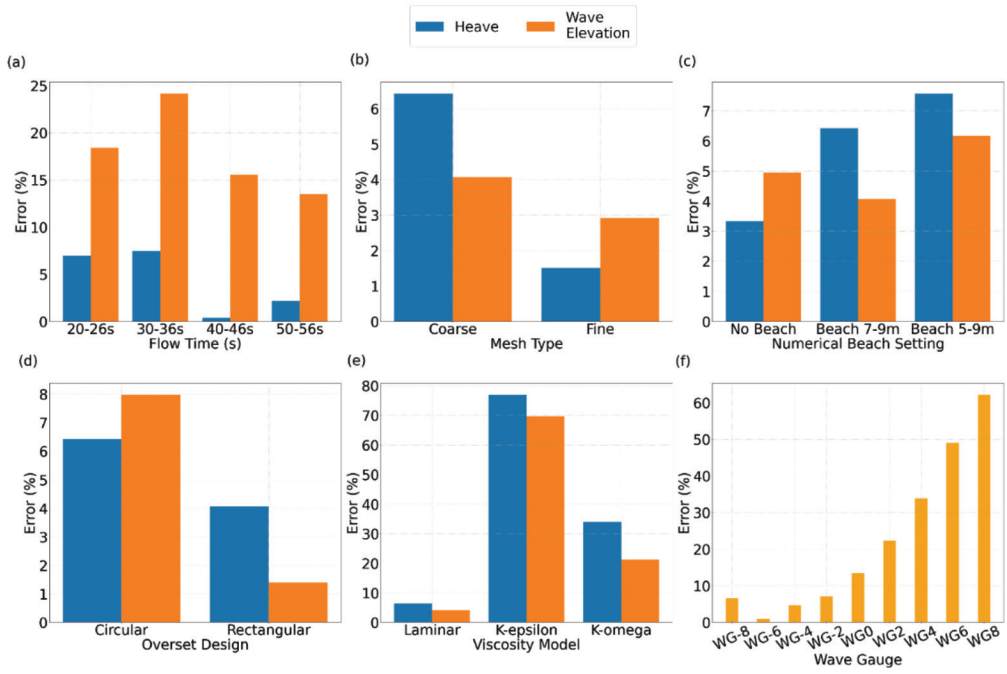

Figure 6. *Comparison of relative error between experimental data [16] and various types of cases for a) time study, b) mesh study, c) numerical beach study, d) overset geometry study, e) viscosity study, and f) spatial study*

This indicates that the experimental conditions produced a flow type that is closer to laminar flow in the wave tank, rather than turbulence. The results also indicate that the SST k-omega model, which is known to be more accurate in modeling near-wall turbulent flow, does a better job than the standard k-epsilon model at replicating flow in the experimental study.

Several previous studies have also demonstrated an accurate replication of experimental results using a laminar model. Zhang et al. [20] used the laminar model and concluded that it was able to predict various phenomena accurately under certain conditions. Zhang et al. [9] used the laminar model to simulate wave propagation on a dual-floater system and found trends similar to those of the experimental data.

Finally, the spatial study, shown in Figures 5f, 5g, 5h, and 6f, shows a high wave elevation before WG0 and continued damping until WG8, because of the beaching effect from the numerical beach. In addition, the offset of wave elevation at downstream locations compared to upstream location intensifies further downstream.

When compared with experimental data, WG-6 shows the most accurate reading, where at WG-8, the amplitude is higher and after WG-6, all values show a lower amplitude than that of experimental data. Downstream of WG0, the amplitude was found to damp more than that upstream of WG0. Location WG0, which shows an error of 13.5%, is considered to be of reasonable accuracy considering the much higher error because of damping for locations WG2-WG8.

3.2. Hydrodynamic Performance

For further study of the numerical model, the most accurate models of independent studies were used, with the same aspects of fixed boundary conditions and NWT dimensions. When a quantitative analysis was conducted using cases of varying wave angular frequencies, the results of heave movement and transmission coefficient, as shown in Figure 7, demonstrated a non-uniform decreasing trend across the ranges of frequencies studied. A valley is observed at wave periods 1.5 s and 1.8 s for heave movement and transmission coefficient, respectively.

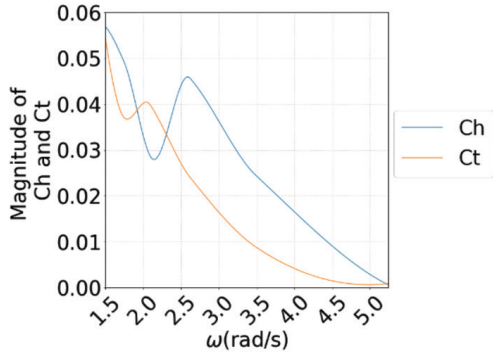

Figure 7. *Comparison of the heave coefficient (Ch) of OB-B and transmission coefficient (Ct) versus wave frequency*

The result of a general decreasing trend in the heave movement of OB across the frequency indicates that more energy can be generated through direct drive when the wave period is longer. This indicates that a location with a higher wavelength and wave period profile is beneficial for wave power generation using OB. Zhang et al. [9], who studied the heave motion of a single WEC with a square bottom, observed a similar trend. A general downward trend across similar frequency ranges, plus the presence of a small valley, is consistent with the result of the heave coefficient of the present study.

Meanwhile, the amount of wave energy transmitted downstream is also generally higher with a longer wave period, which indicates that a lower wavelength and wave period profile is more beneficial for the OB to perform its function as a breakwater.

When the transmission coefficient result is compared to the transmission coefficient at WG2 when OB is absent, the result shows that for a frequency of 2.62 rad/s and a wave period of 1.2 s, models with and without OB have transmission coefficient values of 0.024 and 1.085, respectively. This shows that the OB reduced 97.8% of transmitted wave energy, which makes it an effective floating breakwater that can be used to protect coastal infrastructure. In comparison, only 2% of the incident-wave energy was transmitted in an experimental study of a Berkeley Wedge-shaped floating breakwater by Madhi et al. [21]. This indicates that further improvement to lower the transmitted energy is possible through a geometric optimization approach.

These results are in agreement with the findings of Zhang et al. [9], who studied a dual-floater system where the upstream and downstream buoys are WEC and breakwater, respectively. A general decrease in heave motion and transmission across the wave angular frequency was observed for a single WEC with a square bottom. Another dual-floater system studied by Chen et al. [22] also shows a general decreasing trend across the frequency for all draft ratios.

The results for the vorticity magnitude flow fields are shown in Figures 8 and 9, where the presence of at least one vortex near the front and back edges of the OB is observed for all wave periods except period 0.6 s. The vortex does not increase in size across the wave period and cycle, nor does it increase in intensity. Vortices are phenomena that contribute to energy loss, which then reduces the magnitude of the heave coefficient of the OB. Therefore, solutions such as shape optimization could be implemented for a possible future study.

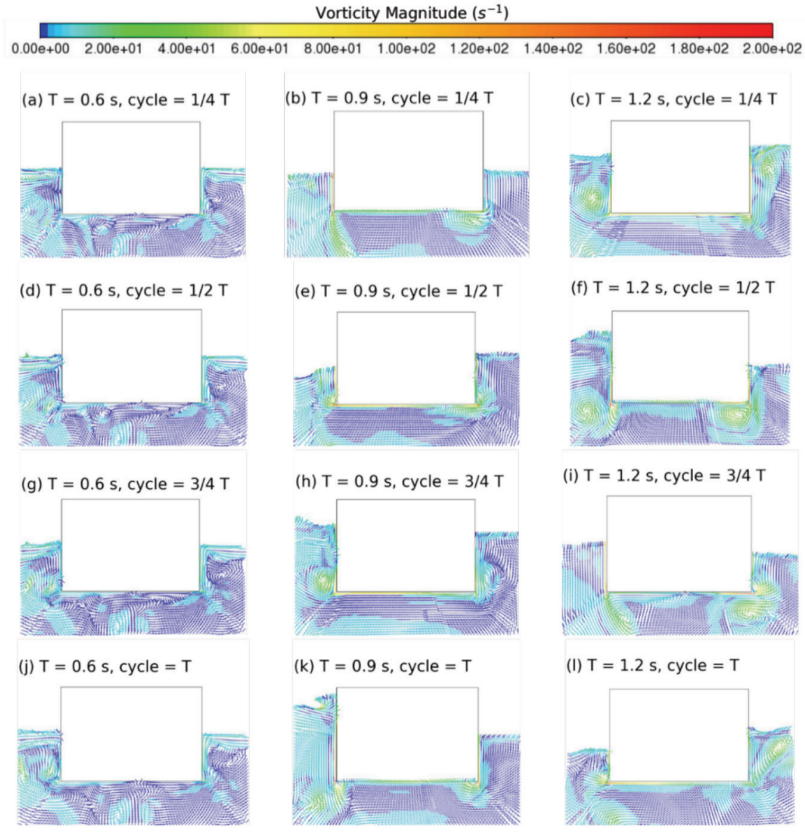

Figure 8. *Flow fields of vorticity magnitude for wave periods 0.6, 0.9, and 1.2 s, for cycles 1/4 T [(a), (e), (i)], 1/2 T [(b), (f), (j)], 3/4 T [(c), (g), (k)], and T [(d), (h), (l)], respectively*

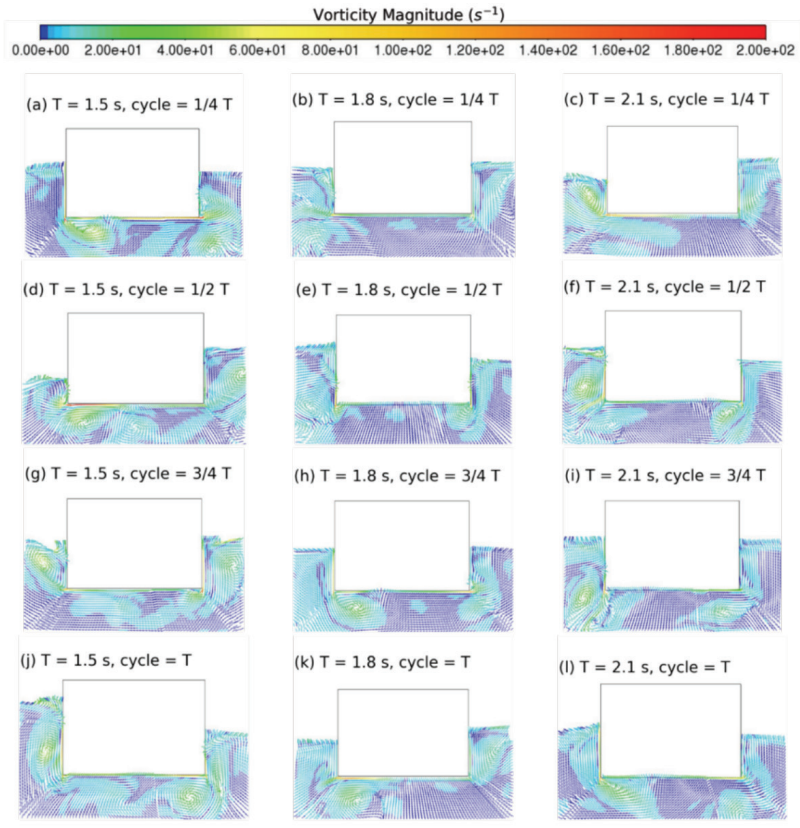

Figure 9. *Flow fields of vorticity magnitude for wave periods 1.5 s, 1.8 s, and 2.1 s for cycles 1/4 T [(a), (e), (i)], 1/2 T [(b), (f), (j)], 3/4 T [(c), (g), (k)], and T [(d), (h), (l)], respectively*

This result is similar to the findings of Zhang et al. [12], who found vortices in the front and back of the studied buoy. In addition, a proposal of a streamlined design of the buoy bottom was made to reduce the flow separations and improve energy conversion, similar to the findings of the present study. When Chen et al. [22] displayed the result of the vorticity magnitude contour of dual-floaters of varied draft ratios, the result showed a higher presence of vortices for models with smaller draft ratios.

4. Conclusion

A study was conducted to create an accurate numerical model and assess the wave conversion and breakwater abilities of an OB. Six independent studies were conducted for the first objective, and three hydrodynamic coefficients were calculated for the second objective.

Some of the limitations of this study are the two-dimensional design of the numerical model, the motion of the OB that is confined to only heave movement, and the assumption of negligible compressibility of air due to the small-scale study.

The findings of this study can be summarized as follows:

Six independent studies were used as validation to derive the ideal numerical setup that replicates the experimental condition at a flow time of 40-46 s for fine mesh setup, 7-9 m numerical beach setting, rectangular overset mesh design, laminar flow viscosity, and location WG0.

Quantitative analysis results for the heave and transmission coefficients show a generally decreasing trend across the wave angular frequency, with a notable presence of a valley at different locations. For the transmission coefficient, the OB was found to eliminate 97.7% of the transmitted wave energy compared to the model without an OB.

Qualitative analysis results of the vorticity magnitude flow field show vortices for all wave periods except the lowest 0.6 s. The vortices appear close to the front and back edges of the OB.

For further studies, geometric optimization of the OB to improve its hydrodynamic performance can be conducted. In addition, the slamming effect on the structural integrity of the OB needs further study to reduce the occurrence of structural failure that increases the cost of maintenance.

Authorship Contributions

Concept design: M. R. A. Rahman, Data Collection or Processing: G. Ram, Analysis or Interpretation: G. Ram, Literature Review: G. Ram, and M. R. A. Rahman, Writing,

Reviewing and Editing: G. Ram, M. R. Saad, N. Z. Abidin, and M. R. A. Rahman.

Funding: The authors declare that no funds, grants, or other support was received during the preparation of this manuscript.

References

[1] N. H. Samrat, N. B. Ahmad, I. A. Choudhury, and Z. Taha, "Prospect of wave energy in Malaysia." In *2014 IEEE 8th International Power Engineering and Optimization Conference (PEOCO2014)*, IEEE, pp. 127-132. Mar 2014.

[2] A. Falcao, "Wave energy utilization: a review of the technologies." *Renewable and Sustainable Energy Reviews,* vol. 14, pp. 899-918, Apr 2010.

[3] W. Sheng, "Wave energy conversion and hydrodynamics modelling technologies: a review." *Renewable and Sustainable Energy Reviews,* vol. 109, pp. 482-498, Jul 2019.

[4] M. Sasson, S. Chai, G. Beck, Y. Jin, and J. Rafieshahraki. "A comparison between smoothed-particle hydrodynamics and rans volume of fluid method in modelling slamming." *Journal of Ocean Engineering and Science,* vol. 1, pp. 119-128, Apr 2016.

[5] Y. Luo, et al. "Numerical simulation of a heave-only floating OWC (oscillating water column) device." *Energy,* vol. 76. 799-806, Nov 2014.

[6] M. N. Gomes, L. A. Isoldi, C. R. Olinto, L. A. O. Rocha, and J. A. Souza. "Computational modeling of a regular wave tank." In *2009 3rd Southern Conference on Computational Modeling*, IEEE, pp. 60-65, Nov 2009.

[7] S. Ringe. *Designing of One Directional Wave Tank*, 2020.

[8] C. Windt, J. Davidson, and J. V. Ringwood. "High-fidelity numerical modelling of ocean wave energy systems: a review of computational fluid dynamics-based numerical wave tanks." *Renewable and Sustainable Energy Reviews,* vol. 93, pp. 610-630, 2018.

[9] H. Zhang, B. Zhou, C. Vogel, R. Willden, J. Zang, and J. Geng. "Hydrodynamic performance of a dual-floater hybrid system combining a floating breakwater and an oscillating-buoy type wave energy converter." *Applied Energy,* vol. 259, pp. 114212, Feb 2020.

[10] P. A. Lakshmynarayanana, *Application of 3D-CFD modelling for dynamic behaviour of ship in waves*., University of Southampton, Apr 2017.

[11] Y. Cheng, et al. "Experimental and numerical analysis of a hybrid wec-breakwater system combining an oscillating water column and an oscillating buoy." *Renewable and Sustainable Energy Reviews,* vol. 169, pp. 112909, Nov 2022.

[12] X. Zhang, Q. Zeng, and Z. Liu. "Hydrodynamic performance of rectangular heaving buoys for an integrated floating breakwater." *Journal of Marine Science and Engineering,* 7, vol. 8, pp. 239, Jul 2019.

[13] Q. Ji, C. Xu, and C. Jiao. "Numerical investigation on the hydrodynamic performance of a vertical pile-restrained reversed l type floating breakwater integrated with wec." *Ocean Engineering,* vol. 238, pp. 109635, Oct 2021.

[14] H. I. Yamac, and A. Koca. "Shore type effect on onshore wave energy converter performance." *Ocean Engineering,* vol. 190, p. 106494, Oct 2019.

[15] K. O. Connell, and A. Cashman. "Development of a numerical wave tank with reduced discretization error." In *2016 International Conference on Electrical, Electronics, and Optimization Techniques (ICEEOT),* IEEE, pp. 3008-3012, Mar 2016.

[16] M. He, B. Ren, and D. Qiu. "Experimental study of nonlinear behaviors of a free-floating body in waves." *China Ocean Engineering,* vol. 30, pp. 421-430, Apr 2016.

[17] S. Lyu, H. Luofeng, and T. Giles. "Motions of a floating body induced by rogue waves." OpenCFD Limited, Jul 2019.

[18] B. LeMéhauté. *An introduction to hydrodynamics and water waves*. *Environmental Science Servies Administration*, vol. 52, pp. 205, 1969.

[19] S.-C. Jiang, W. Bai, and G.-Q. Teng. "Numerical simulation of wave resonance in the narrow gap between two non-identical boxes." *Ocean Engineering,* vol. 156, pp. 38-60, May 2018.

[20] H. Zhang, S. Liu, M. C. Ong, and R. Zhu. "CFD Simulations of the propagation of free-surface waves past two side-by-side fixed squares with a narrow gap." *Energies*, vol. 12, pp. 2669, Jul 2019.

[21] F. Madhi, M. E. Sinclair, and R. W. Yeung. "The "berkeley wedge": an asymmetrical energy-capturing floating breakwater of high performance." *Marine Systems & Ocean Technology*, vol. 9, pp. 5-16, Jun 2014.

[22] L. Chen, X. Cao, S. Sun, and J. Cui. "The effect of draft ratio of side-by-side barges on fluid oscillation in narrow gap." *Journal of Marine Science and Engineering,* vol. 8, pp. 694, Jul 2020.